HALALSPHERE
International Islamic University Malaysia - INHART

Conventional Blending Chitosan Lignin Nanocomposites Hydrogel (CsLNPs) for food coating application

Amelia Shanaz Ahmad Tarmizi[a,b], Muhammad Bisyrul Hafi Othman[a,b,*], Muhamad Shirwan Abdullah Sani[c], Nur Najmina Rafiae[a,b], Nur Raihan Rostan[a,b], and Mohamad Nasir Mohamad Ibrahim[a,b]

[a]School of Chemical Sciences, Universiti Sains Malaysia (USM), 11800 Penang, Malaysia.
[b]Materials Technology Research Group (MaTRec), School of Chemical Sciences, Universiti Sains Malaysia (USM), 11800 Minden, Penang, Malaysia.
[c]International Institute for Halal Research and Training (INHART), Level 3, KICT Building, International Islamic University Malaysia (IIUM), 53100 Kuala Lumpur, Malaysia.
*Corresponding author: E-mail address: bisyrul@usm.my

Received:21/11/2024
Accepted:16/1/2025
Published:31/1/2025

Keywords:
Chitosan (Cs) hydrogel; Lignin nanoparticles (LNPs); Thermal stability; Food coating; Food security

Abstract

Despite the importance of bio-based materials for food coatings, studies on how LNPs enhance thermal stability, swelling behaviour, and barrier properties remain limited, creating a gap in sustainable food preservation solutions. This work successfully prepared the lignin chitosan nanocomposites hydrogel (CsLNPs) via a conventional, cost-effective blending method. The incorporation of LNPs into Cs hydrogels was confirmed via FTIR, showing interactions between LNPs' -OH groups and Cs' -NH2 groups, with peak shifts at 3400–3200 cm^{-1}. Thermal analysis revealed decomposition temperatures (T_{max}) of 285–290°C, with T10% >170°C and >24% residue at 800°C. Glass transition temperatures (Tg) ranged from 143–154°C. LNPs initially improved thermal stability, although higher loading caused agglomeration, reducing performance. LNPs-Cs hydrogels displayed insolubility in non-polar solvents due to their inherent structure, while increasing lignin loading (5–20%) enhanced water absorption and swelling, slowing fruit rotting. This demonstrated improved moisture and oxygen barrier properties. The findings highlight CsLNPs as a sustainable, effective food coating, reducing waste, promoting eco-friendly packaging, and advancing bio-based solutions for food technology.

1. Introduction

In recent years, there has been a growing global emphasis on sustainable consumption and production practices to address pressing challenges such as food security (Vågsholm *et al.*, 2020) and environmental sustainability. Among various strategies, developing biocompatible materials for food packaging (Rai *et al.*, 2017) and coating applications (Rafiae *et al.*, 2024) stand out as a pivotal area for innovation. Biopolymers derived from renewable resources offer promising solutions due to their biodegradability, low environmental impact, and potential to enhance food preservation and safety (Munteanu & Vasile, 2020). This activity is particularly crucial in improving the safety and quality of perishable foods during storage and transportation, thereby addressing food security challenges. As regulatory frameworks worldwide increasingly prioritise sustainable packaging materials and food safety standards, biopolymers offer compliant solutions that align with consumer preferences for eco-friendly products.

Chitosan (Cs) is a natural polysaccharide derived by the partial deacetylation of chitin, a structural component found in crustaceans' exoskeletons (Nasrollahzadeh *et al.*, 2021). Their integration into nanocomposite hydrogels presents a compelling approach towards sustainable food coating applications. Cs, known for their antimicrobial properties and biocompatibility, can prolong the shelf-life of perishable foods by inhibiting microbial growth (Souza *et al.*, 2020). With its robust structural properties and antioxidant capabilities, lignin complements Cs by enhancing mechanical strength and providing additional barrier protection against oxygen and moisture. These allow for improved compatibility with various polymeric matrices, expanding the scope of CsLNPs composite materials across diverse fields, including wastewater treatment (Sohni *et al.*, 2019), food packaging (Rai *et al.*, 2017), and tissue engineering (Islam *et al.*, 2020). Moreover, amidst global challenges related to food security, where efficient food preservation and distribution are crucial, the development of CsLNPs holds promise in enhancing food safety and extending shelf life. By exploring the formulation and performance of CsLNPs as food coatings, this research contributes to the broader objective of achieving sustainable food systems that are resilient, resource-efficient, and environmentally responsible.

Chemical approaches like cross-linking and polymerisation involve potentially toxic agents and raise environmental concerns. They also present difficulties in achieving uniform particle sizes. Self-assembly poses challenges in maintaining consistent particle size and scalability (Hussin *et al.*, 2022). Solvent-based methods, such as solvent shifting and acid

precipitation, require careful solvent selection and may contribute to environmental and safety issues (Hussin *et al.*, 2022). Zhang *et al.*, 2021, reported that carbon dioxide antisolvent precipitation demands specialised equipment and introduces safety considerations due to high-pressure CO2. Lastly, physical methods like ultrasonication may encounter issues such as agglomeration and difficulties in achieving uniform particle sizes, with ultrasonication potentially generating heat that can alter Nanolignin properties (Tang *et al.*, 2020).

These disadvantages underscore the need for alternative, more efficient methods in LNPs preparation. Moreover, assessing the hydrogel's biocompatibility may involve complex and time-consuming biological assays, introducing challenges in standardisation and reproducibility. The analysis of degradation properties could be hindered by the diverse environmental conditions encountered during degradation testing, making it difficult to draw conclusive comparisons. These disadvantages underscore the need for careful consideration and standardised methodologies when investigating the influence of Nanolignin content in nanocomposite hydrogels.

This work focuses on obtaining Cs lignin nanocomposite hydrogels (CsLNPs) with the lignin nanoparticles (LNPs) extracted from the Empty Fruit Bunches (EFB) of oil palm. The LNPs were prepared using the high shear homogenisation method to increase dispersion and thermal resistance, while Cs/LNPs were mixed under an ambient environment using a conventional blending technique. To our knowledge, this is the first instance of developing a simple nanocomposite hydrogel that significantly extends the shelf life of fruits and vegetables by preventing oxidation and rapid deterioration, thus addressing the growing demand for eco-friendly coating solutions. Using shear homogenisation—which applies mechanical shear forces through high-speed rotating blades or narrow gaps—effectively reduces particle size and creates emulsions.

2. Materials and methods

2.1 Materials

Oil Palm Empty Fruit Bunch (EFB) supplied by the LignoTek Lab, School of Chemical Sciences, USM. Sodium hydroxide (NaOH, 30%) from Progressive Scientific Sdn. Bhd. Sulfuric acid (H2SO4, 98%) was purchased from Avantor Performance Materials Llc. Chitosan (Cs) powder was bought from Xi'an Lanshan Biotechnology Co., Ltd., While an acetic acid (CH3COOH, 2%) was supplied from QREC (ASIA) Sdn. Bhd. Distilled water and deionised water were also used in the study.

2.2 Preparation of Lignin Nano Particles (LNPs)

Lignin was extracted from the empty palm oil fruit bunch (EFB) using a soda pulping technique. The empty fruit bunch (EFB) was treated with 30% sodium hydroxide (NaOH) at 170°C for 3 hours. The resultant black liquor was vacuum-filtered to remove excess pulp residues (degraded carbohydrates and inorganic ions). The lignin was separated by progressively acidifying the black liquor to pH 2 with 20% v/v H2SO4 solutions. The precipitated lignin was centrifuged at 3500 rpm for 10 minutes to remove excess water, then dried in an oven at 45°C for 48 hours to remove moisture before being ground to a fine brown powder.

About 4 g of soda lignin was soaked and dispersed in 400 mL of deionised water. Then, it was treated at four different shear speeds of the homogeniser (mechanical homogeniser, IKA T25 digital ULTRA-TURRAX, USA with IKA) for 1 hour and then was sonicated using an ultrasonic bath sonicator for 10 minutes. Finally, the samples were dried using a freeze-dried method at around 45°C. Table 1 summarises a series of LNPs prepared at different homogeniser speeds.

Table 1: Summary of the preparation of LNPs for four different homogeniser speeds

Sample designation	Homogeniser speeds (rpm)	pH	t(min)
LNPs6	6400	2	60
LNPs8	8400	2	60
LNPs10	10400	2	60
LNPs12	12400	2	60

2.3 Preparation of lignin chitosan nanocomposites hydrogel (CsLNPs)

About 10 g of Cs was individually dissolved in an acetic acid solution (2%, 90 mL) with stirring at 500 rpm for 3 hours to yield the Cs solution. Simultaneously, LNPs 0.5 g was dissolved in deionised water (9.5 mL) at 500 rpm for 3 hours to produce the LNPs solution (5 wt%). The Cs solution (10 g) and Nanolignin solution (10 g) were mixed and stirred at 1000 rpm for 3 hours. Then, the homogeneous mixture was cast into a petri dish and thawed at room temperature for 3 days. The CsLNPs series are shown in Table 2.

Table 2: Summary of the preparation of CsLNPs hydrogel series

Hydrogel Sample	**Mass of Cs (g)**	**Mass of LNPs (g)**	**LNPs Loading (%)**
Cs	10.0	0	0
CsLNPs 5%	9.5	0.5	5
CsLNPs10%	9.0	1.0	10
CsLNPs20%	8.0	2.0	20
NLPs	0.0	10.0	100

2.4 Characterisation

2.4.1 Fourier Transform Infrared-Attenuated Total Reflectance Spectroscopy (FTIR-ATR)

The FTIR spectra of LNPs and CsLNPs were obtained using Perkin Elmer System 2000 (Perkin Elmer Norwalk, USA) at the frequency range of 4000 cm^{-1} to 400 cm^{-1} with a resolution of 8 cm^{-1} and 32 scans.

2.4.2 Ultraviolet-Visible Spectroscopy (UV-Vis)

UV-Vis spectra were obtained using SHIMADZU UV-Vis-2600i Spectroscopy (SHIMADZU, USA). Samples were placed in a cuvette calibrated using distilled water as a blank solution, and the absorbance and transmittance over a wavelength range of 100 to 1000 nm were measured.

2.4.3 Thermal properties

A Perkin Elmer TGA STA 6000 (TA Instruments, New Castle, USA) thermogravimetric analyser was used for thermogravimetric analysis (TGA). Nitrogen was used as a purge gas with a 40 mL/min flow rate. About 10 mg of samples were heated at 10 °C/min from 25 °C to 800 °C.

Differential Scanning Calorimetry (DSC) analysis was used to analyse the sample glass transition temperature (Tg) and heat capacity variations using DSC Netzsch 3500 Sirius (Netzsch, Germany). About 10 mg of samples were heated at 10 °C/min from 25 °C to 200 °C under a 25 mL/min nitrogen flow rate.

2.4.4 Chemical stability

A solubility test was conducted by dissolving each of the 5 mm x 5 mm samples in 10 mL of 1.0M sulfuric acid (H_2SO_4), 1.0M acetic acid (CH_3COOH), 1.0M sodium hydroxide (NaOH), 1.0M ammonia (NH_3), chloroform, dimethylformamide (DMF), and hexane, which represent the respective strong acid, weak acid, strong base, weak base, protic, polar aprotic, and non-polar solvents under ambient condition.

The degree of swelling was determined using the swelling test. The mass of 5 mm x 5 mm of dry samples were accurately recorded (Wtdry) and immersed in deionised water (pH = 7.2) at 25°C. The wet mass was recorded (Wt_{wet}) each hour until 25 hours. The degree of swelling was calculated according to Eq. 1:

$$\text{Degree of Swelling (\%)} = \frac{Wt_{wet} - Wt_{dry}}{Wt_{dry}} \text{ x } 100\% \qquad \text{Eq. 1}$$

where, Wt_wet represents the final mass of the sample after immersion while Wt_dry represents the initial mass of the sample before immersion.

2.4.5 Pre-coated banana analysis

To assess the effectiveness of Cs hydrogel, LNPs hydrogel, and varying concentrations (5%, 10%, 20%) of the CsLNPs hydrogel as fruit preservation and in extending the shelf-life and preserving the quality of unripe bananas, a controlled experiment was conducted. Unripe banana samples were divided into groups: one uncoated (control) and others coated with the specified hydrogel formulations using the dip coating method, ensuring uniform coverage. The coated bananas were then stored under controlled environmental conditions, and the colour and appearance change pictures were taken daily over 7 days of deterioration. The study aimed to evaluate which hydrogel formulation, if any, effectively delayed the ripening process and maintained banana quality over time.

3. Results and discussion

3.1 Fourier Transform Infrared-Attenuated Total Reflectance Spectroscopy (FTIR-ATR)

The FTIR spectra of the LNPs series prepared at different homogeniser speeds in the range of 500-4000 cm^{-1} are presented in Figure 1. The characteristic absorption bands for LNPs were indicated by the presence of peaks at the 3421 cm^{-1} (O-H stretching), 1600–1500 cm^{-1} (skeletal vibrations of lignin aromatic rings) and 1107 cm^{-1} (aromatic and ether stretching) (Yaqoob *et al.*, 2021). The spectra demonstrated that preparing LNPs at different homogeniser speeds did not alter the lignin functional groups. This finding is consistent with Rahman *et al.*, 2018, who reported that the functional groups of nanosized lignin are similar to those of pristine lignin. However, as the homogenisation speed increases from 6400 to 12400 rpm/h, the peaks at 3400–3200 cm^{-1} (O-H stretching), 1600 cm-1 (C-H stretching of aromatic rings), and 1212 cm-1 (C-O stretching) show decreased intensity, which is suggested to be due to the reduction of LNPs' size and increased surface interactions between LNPs. This result is consistent with the work reported by Sekeri *et al.*, 2020, which is the fragmentation and alteration of lignin's molecular structure, creating smaller units that expose more aromatic rings that enhance the absorbance of LNPs spectra. The FTIR spectra of Cs hydrogel and LNPs displayed distinctive absorption bands, as shown in Figure 2.

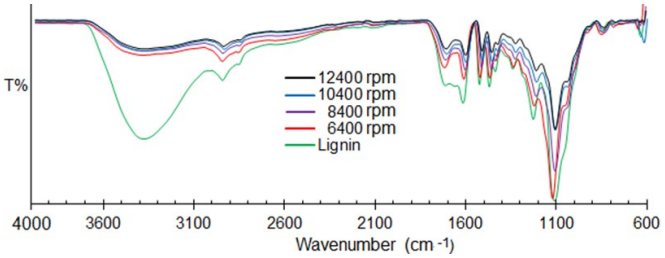

Figure 1: FTIR spectra of LNPs series prepared at different homogeniser speeds.

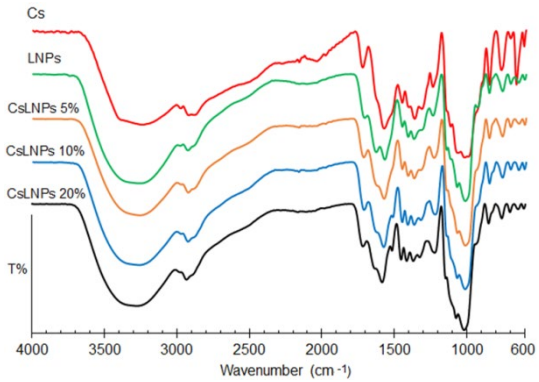

Figure 2: FTIR spectra of CsLNPs hydrogel series.

Cs exhibits a broad absorption band at around 3400-3200 cm^{-1} (stretching vibrations of O-H and N-H groups), 2920-2850 cm^{-1} (C-H stretching of methylene groups) and 1577.38 (amide II, N-H bending vibrations) which are characteristic of the Cs polymer backbone (Mohamad Zharif *et al.,* 2021). Introducing LNPs in Cs hydrogel in the form of CsLNPs hydrogel series exhibit shifted distinctive absorption bands at 3289.86 cm^{-1} (broad O-H and N-H stretching), 2932.27 cm^{-1} (C-H stretching), 1634.05 cm^{-1} (amide I) and 1575.63 cm^{-1} (amide II). These peak findings are consistent with what was reported by Mohaiyiddin *et al.,* 2018. These findings suggest that the -OH in LNPs interaction with $-NH_2$ in Cs hydrogel through electrostatic interaction leads to the shifted peak in the Cs LNPs hydrogel series without the disappearance of the Cs hydrogel peaks attribute. (Figure 3).

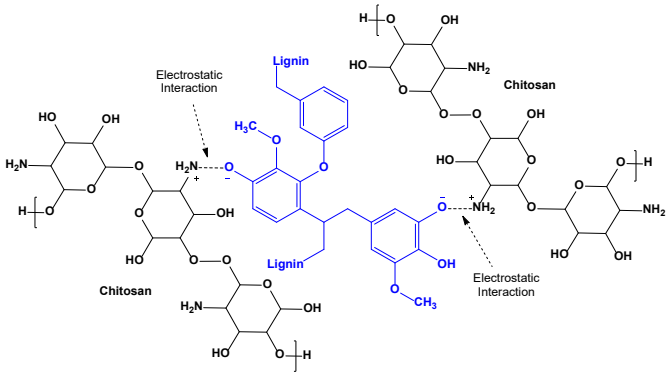

Figure 3: The electrostatic interaction between LNPs and Cs molecules.

Amino groups (-NH2) in Cs hydrogels can be protonated in acidic conditions, imparting a positive charge along the Cs chains, while hydroxyl (-OH) groups in LNPs deprotonated under neutral to basic conditions, giving the lignin nanoparticles a negative charge. As Cs hydrogel and LNPs were brought into contact in an aqueous environment, electrostatic interactions occurred between the positively charged amino groups on Cs and the negatively charged hydroxyl groups on lignin. These suggested that electrostatic attractions can facilitate the dispersion of lignin nanoparticles within the Cs hydrogel matrix, especially at lower concentrations of LNPs. As the loading of hydroxyl lignin nanoparticles increases, positively charged Cs hydrogel can become overwhelmed by the negatively charged LNPs and increase the tendency for LNPs to aggregate or agglomerate. This leads to phase separation within the Cs hydrogel matrix, where regions enriched with LNPs form distinct clusters or domains. Later, this creates stress concentration points or weak interfaces within the CsLNPs hydrogel matrix, which affects its overall thermal and mechanical stability.

3.2 Ultraviolet-Visible Spectroscopy (UV-Vis)

UV-Vis analysis studies the interactions between LNPs and Cs molecules within the CsLNPs hydrogel series, especially the bonding between the hydrogel matrix. Figure 4 shows the loading-dependent spectra of CsLNPs hydrogel measured in distilled water at room temperature.

LNPs show a prominence absorbance peak at 285 nm and a weak shoulder at 280 – 320 due to their aromatic ring structures and conjugated double bonds. Cs shows a broad and weak shoulder at the wavelength 280 – 320 nm due to partially deacetylated chitin forming carbonyl-containing degradation products (Rai *et al.,* 2017). The absorbance peak was less intense in Cs hydrogel due to it lacking conjugated double bonds, which had strong n→π* and π→π* electronic transitions that absorb UV light.

The increasing 5% LNPs loading results in more LNPs within the CsLNPs hydrogel matrix. This result suggested that the overall absorption of light passing through the CsLNPs hydrogel matrix was enhanced (Rai *et al.,* 2017). This result was consistent with Beer's Law, which states that absorbance is directly proportional to the concentration of the absorbing species—further increasing to 20% LNPs loading results in increasing absorbance proportionally. The formation of charge transfer complexes between lignin and Cs could also increase absorbance and intensify the peak at the wavelength 285 nm.

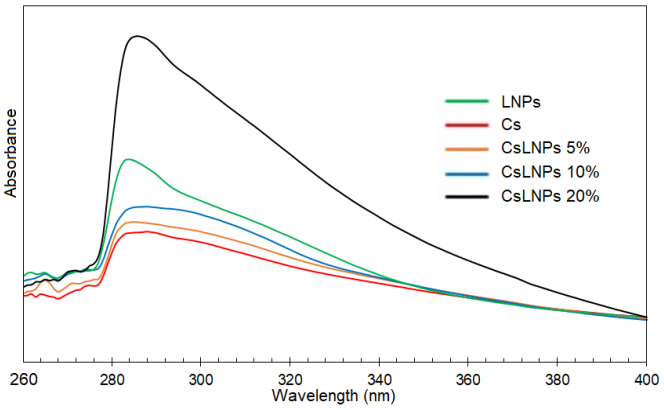

Figure 4: UV-Vis spectra of CsLNPs hydrogel series.

As the loading of hydroxyl lignin nanoparticles increases, positively charged Cs hydrogel increases, leading the LNPs to aggregate or agglomerate, increasing absorbance.

3.3 Thermal properties

TGA provides valuable information on thermal stability, decomposition kinetics, and material composition by measuring mass changes with temperature, making it particularly useful for assessing CsLNPs hydrogel series degradation. Figure 5 shows that the CsLNPs hydrogel series exhibited a one-step degradation with an onset temperature of around 100 °C to an end-set temperature of around 400°C. In comparison, LNPs hydrogel showed a two-step degradation: the first at 310°C and the second was above 450°C. LNPs hydrogel has demonstrated higher thermal decomposition temperature (T_{max}) than Cs hydrogel due to the complexity of lignin molecules, which is cross-linked aromatic or branched with strong covalent bonds; in contrast, Cs hydrogel has a more linear structure with less cross-linking, leading to lower thermal stability. Besides that, the presence of aromatic rings in lignin molecules causes slower and more gradual mass loss and withstand higher temperatures before breaking down, leaving higher char once degradation ends at 800 °C. Cs decomposed more rapidly at lower temperatures due to their less stable amine and hydroxyl group structure, which often degrades as volatile compounds like water (Vasilev *et al.,* 2019). Table 3 shows that Cs hydrogel has about 10% less char than LNPs hydrogel.

Increasing LNPs loading from 10% to 20% in CsLNPs hydrogels shows that T_{max} does not significantly reduce thermal decomposition. This result suggested that complex aromatic structures and strong covalent bonds in lignin molecules are inherently thermally stable, preventing a substantial decrease in the thermal degradation temperature. Table 3 also proved that increasing LNPs loading promoted higher char formation during decomposition, which protects against further degradation. Besides that, T_{max} contributed to the Cs fraction; as the lignin loading increased, which led to more char, the Cs fraction decreased, leading to a decrease in T_{max}. Therefore, CsLNPs hydrogels exhibit synergistic effects with component fraction in the hydrogel, enhancing the overall thermal stability beyond what would be expected from simply increasing the amount of lignin alone.

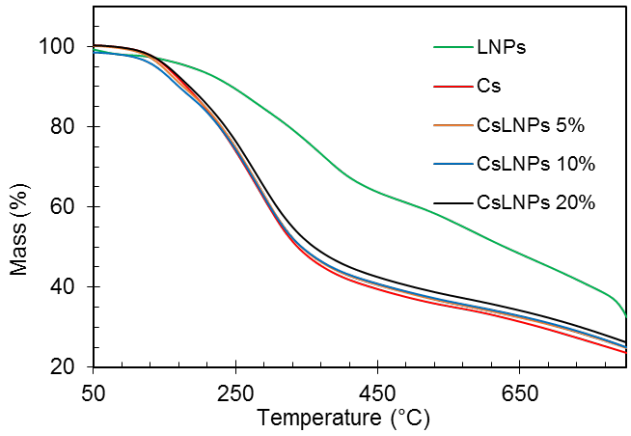

Figure 5: TGA and DTG curves for CsLNPs hydrogel series.

The DSC curves, recorded on the second heating cycle (Figure 6), determine the CsLNPs chain mobility. The shift in temperature was related to the interactions between the Cs matrix and the lignin nanoparticles. The traces of the Cs molecules in Cs hydrogel 0% were seen at the first endothermic peak, at 110–130°C, which was attributed to absorbing moisture. In contrast, Cs's glass transition temperature (Tg) is 120°C. This value is slightly lower than Cs thin film (Tg=140 - 150°C), which has been reported by Dong *et al.* 2004, due to Cs hydrogel having a strong affinity towards water (water-polymer interaction). Their endotherm is usually related to water's evaporation, which was observed to be lower than Cs thin films. Introducing 5% LNPs in CsLNPs hydrogel using a blending technique shows Tg increases around 30°C. This suggested that the 5% LNPs increase the rigidity of the Cs backbone while restricting the mobility of Cs molecules to soften at higher temperatures (Noor *et al.,* 2020).

Table 3: TGA and DTG results for CsLNPs hydrogel series

Hydrogel Sample	**T_{10}**	T_{max}	**Residue at 800 ˚C**
Cs	180.5	290.4	23.6
CsLNPs 5%	175.5	290.5	24.8
CsLNPs 10%	170.8	285.8	25.0
CsLNPs 20%	185.5	285.5	26.2
LNPs Hydrogel	245.5	365.5	32.5

Further increasing to 20% LNPs in CsLNPs hydrogel, the thermal stability of the CsLNPs hydrogel series did not continue to increase. Instead, it has a negative effect, causing the Tg to drop 10°C to 143°C. This result suggested that the LNPs may start to agglomerate, leading to poorer dispersion within the Cs matrix while increasing the free volume within the polymer matrix, which can facilitate molecular motion and lower the Tg. The initial increase in Tg at 5% LNPs can be explained as well-dispersed LNPs, meaning they are uniformly distributed throughout the Cs hydrogel matrix. This increase facilitated a good interaction between LNPs and Cs chains, restricting chain mobility. Janik *et al.,* 2021, reported that decreasing free volume significantly increases the Tg.

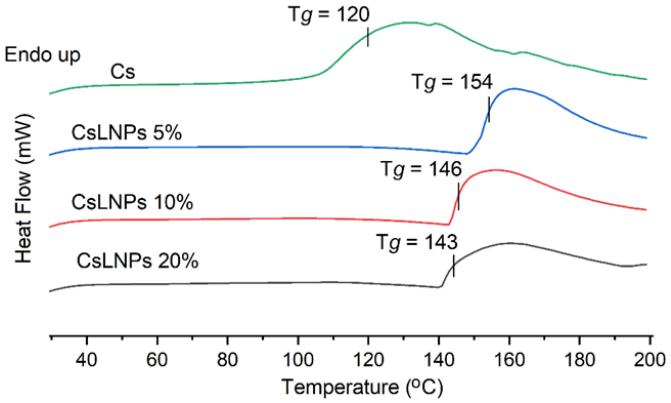

Figure 6: DSC curves for CsLNPs hydrogel series.

This result was contrary to further increasing LNPs loading, which induced LNPs to agglomerate, creating non-uniform regions to lead aggregates. In contrast, the increased free volume allows molecular motion and decreases Tg. Although Tg showed a decreasing trend, this was not always consistent with the decreasing trend in materials stability. Figure 7 shows the correlation between chain mobility and thermal decomposition temperature of the CsLNPs hydrogel series.

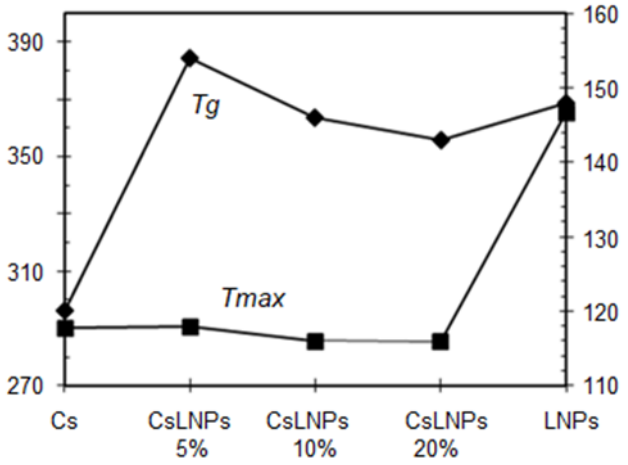

Figure 7: Correlation between Tg and T_{max} CsLNPs hydrogel series.

Introducing 5% LNPs in CsLNPs hydrogel using a blending technique shows the increases in Tg but on T_{max}. This result suggested that T_{max}, the temperature at which significant decomposition of the hydrogel occurs, is primarily governed by the thermal properties of lignin. The addition of LNPs does not significantly alter the overall thermal stability of the hydrogel and initially ensures a homogeneous distribution of nanoparticles, which allows lignin to exert its reinforcing effects evenly throughout the hydrogel matrix, influencing the mechanical and thermal properties consistently; hence, the T_{max} remains unchanged. At higher loadings of LNPs, like 10%, agglomeration or uneven dispersion of LNPs can exacerbate phase separation and reduce the effectiveness of lignin in reinforcing the hydrogel structure. This uneven distribution can lead to inconsistent thermal properties across the hydrogel, affecting Tg and T_{max}.

3.4 Chemical stability

To be used in food coating applications, determining the chemical stability of CsLNPs hydrogel series in various solvents is crucial due to the chemical resistance and durability of materials, solubility and interaction materials with food components, food safety and shelf life, and fulfilment of the regulatory compliance. These results help optimise the hydrogel for real-world food applications, ensuring it meets industry standards and consumer expectations. The solubility behaviour of the CsLNPs hydrogel series compared to the results of the LNPs hydrogel and Cs hydrogel can be found in Table 4.

LNPs hydrogel is fully soluble in strong bases, weak acids, and weak bases, except for the strong acids. Zhang *et al.,* 2021, reported that Cs-lignin composites resisted strong acids. On the other hand, Cs hydrogel was partially soluble in similar acidity/basicity environments. This result is due to the amino groups ($-NH_2$) in Cs molecules either becoming protonated to form $-NH_3^+$ ions at pH<6 or deprotonated at pH>7, resulting in the formation of $-NH_2$, which leads to increased or decreased electrostatic repulsion between chains, which helps to dissolve/aggregate the Cs in the acidic/basic solution—introducing LNPs hydrogel in a Cs hydrogel system through conventional blending, resulting in the CsLNPs hydrogel series exhibiting partial solubility. Further, increasing LNPs loading does not change partially soluble behaviour. This result suggested that the composite hydrogel does not dissolve as completely as lignin hydrogel does on its own but behaves more like Cs regarding solubility. As the system molecular weight of Cs increases due to the interaction with LNPs molecules, chain length and entanglement may increase, leading to more significant aggregation and lower solubility.

LNPs and CsLNPs hydrogel series demonstrate insoluble behaviour in non-polar solvents due to their inherent chemical structure and the nature of non-polar solvents. Note that the hydroxyl (-OH) groups and amino groups ($-NH_2$) can form hydrogen bonding and be protonated. Non-polar solvents lacking in polarity characteristics (partial positive or negative charges) form hydrogen bonds or engage in this interaction to dissolve Cs and lignin segments (Mohaiyiddin *et al.,* 2018). Almost a similar reason can be applied to the polar aprotic solvent which has been utilised. Thus, it can be justified that using water, ethanol, and acetic acid is most suitable in the hydrogel preparation process to meet the requirements of regulatory agencies for green materials. Due to the water existing in the air as a moister, swelling tests are essential for determining the chemical stability of CsLNPs hydrogel series to provide insights into moisture control, structural integrity coating material, compatibility with food environments, process optimisation, and safety. Figure 8 shows swelling result of CsLNPs hydrogel series in water for 25 hours.

The characteristic of Cs hydrogel swelling degree has been demonstrated as the water uptake rapidly raised during the first 4 hours. This result is due to the efficiency of hydrophilic (hydroxyl, -OH) groups in Cs molecules, which quickly attract water to be absorbed. Then, the intrinsic porous structure of the CsLNPs hydrogel frameworks facilitates the capillary action, which allows water molecules to penetrate the network quickly during the initial phase, causing the hydrogel to swell rapidly. After the initial rapid swelling, at the 5th hour, the hydrogel reaches a saturation point, indicating that water molecules fully occupy the internal hydrophilic sites. At this point, the Cs hydrogel framework reaches a state of equilibrium where the osmotic pressure inside the hydrogel balances with the external water pressure through the hydrogen bonding and van der Waals forces, stabilise the hydrogel structure, preventing further water uptake from maintaining a constant degree of swelling.

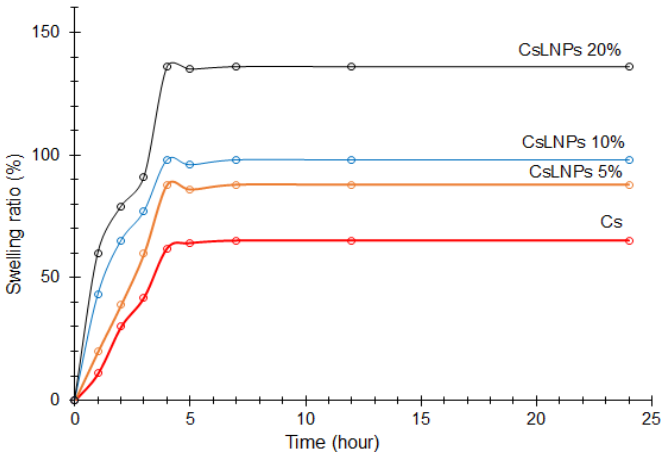

Figure 8: Swelling result of CsLNPs hydrogel series in water for 25 hours.

The increased lignin loading from 5% to 20% in the CsLNPs hydrogel series has significantly increased the swelling. This result suggested that the nature of lignin (-OH group) increases the overall hydrophilicity of the hydrogel, which enhances an ability to absorb and retain more water molecules, leading to increased swelling. Besides, with higher lignin content, the hydrogen bonds become more efficient in creating a more open hydrogel framework. This increases the free volume or spacing between Cs molecules and a higher swelling (Mohaiyiddin *et al.,* 2018). Therefore, as the water absorption capacity is maximised in higher lignin loading, the equilibrium state is also maximised before further expansion is prevented. The results conclude that the CsLNPs hydrogel series demonstrate that the maximal loading of NLPs applied maximal swelling behaviour, which indicates good green coating barrier

Table 4: Solubility of CsLNPs hydrogel series.

Hydrogel Samples	H_2SO_4 Strong acid	NaOH Strong base	AcOH Weak acid	NH_3 Weak base	$CHCl_3$ Polar protic	DMF Polar aprotic	Hexane Non-polar
Cs	±	±	±	±	±	-	-
CsLNPs 5%	±	±	±	±	-	-	-
CsLNPs 10%	±	±	±	±	±	-	-
CsLNPs 20%	±	±	±	±	±	±	-
LNPs	-	+	+	+	-	+	-

soluble: +, partially soluble: ±, insoluble: -

properties, which is essential for extending the shelf life of food products at the same time easily be removed by rinsing with water tap.

3.5 Pre-coated banana analysis

In this segment, the evaluation of pre-coating fruit shelf-life critically examined the CsLNPs hydrogel series to ensure that the coating process meets quality standards, such as uniformity, thickness, and adherence (Munteanu & Vasile, 2020). The coating provides a barrier against moisture loss, oxidation, and microbial growth. The results stemmed from a 7-day observation of bananas treated with the CsLNPs hydrogel solution, illustrated in Figure 9.

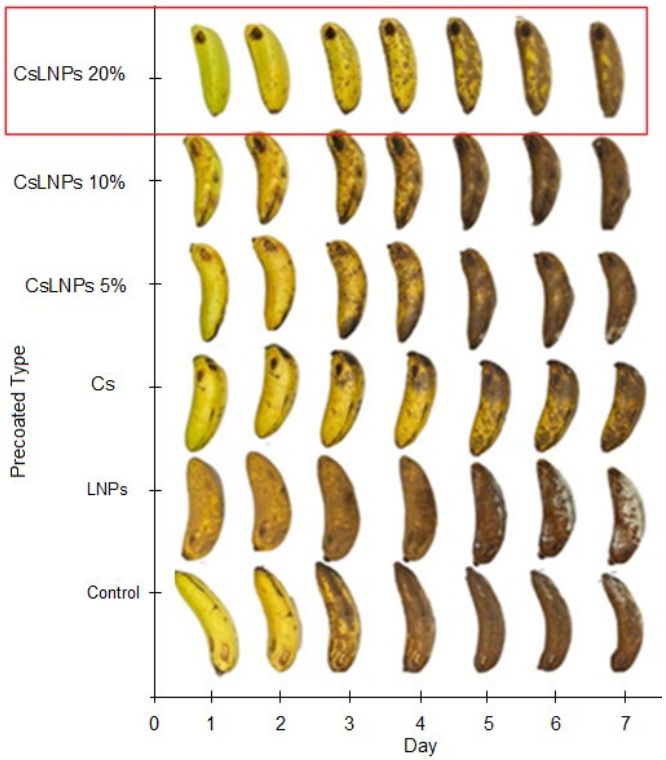

Figure 9: Pre-coated banana shelf-life analysis of CsLNPs hydrogel series.

Pre-coated bananas with LNPs hydrogel demonstrate faster deterioration and mould growth than uncoated bananas. This result suggests that abundant hydroxyl groups in the lignin molecule structure increase moisture retention on the banana's surface (acting as a nutrient source), creating a conducive environment for certain fungi (Souza *et al.,* 2020). Although lignin has antimicrobial properties, it is not strong enough to effectively prevent mould growth, especially in high moisture levels. On the other hand, Pre-coated bananas with Cs hydrogel demonstrated rotting without mould growth due to their antimicrobial properties, which can inhibit the growth of moulds/pathogens by disrupting microbial cell membranes and interfering with microbial metabolism. Besides that, Cs form a more effective barrier against moisture/oxygen and help to regulate moisture more effectively than lignin.

Introducing 5% of LNPs in CsLNPs hydrogel might minimally contribute to the overall properties of the hydrogel. The small amount of LNPs suggested slightly altered the barrier and antimicrobial properties by disrupting the chitosan matrix, leading to faster deterioration than Cs and making it less effective in mould growth. As the LNPs loading increased to 10%, it still demonstrated some deterioration, further reducing the mould growth, suggesting that due to the contribution of enough electrostatic interaction between LNPs and Cs in the CsLNPs hydrogel matrix.

The increases in lignin loading from 20% in the CsLNPs hydrogel series exhibit a slower rotting process. This result suggested that the lignin molecules are hydrophobic, and their integration into the Cs matrix enhanced the effective barrier properties against moisture and oxygen. Next, oxygen permeability is reduced, the respiration rate of the bananas slows down, and the ripening/ rotting process is delayed (Munteanu & Vasile, 2020). CsLNPs20% hydrogel demonstrated almost similar rotten performance to pure Cs hydrogel, indicating a balanced and effective combination of chitosan and lignin properties. Besides that, the mechanical strength and stability of CsLNPs20% molecular framework are enhanced due to more hydrogen bonding interaction between –OH and NH_2 group in lignin Cs hydrogel. The uniformity of coating assisted in ensuring consistent protection across the entire surface of the banana. The enhancement of mechanical strength in hydrogel molecular framework well-adhered with thermal stability. This result highlights the importance of selecting appropriate coating materials based on their interaction with food products and protective capabilities.

4. Conclusion

The CsLNPs were successfully prepared via a conventional blending method, highlighting the feasibility of integrating lignin nanoparticles (LNPs) into Cs hydrogel matrices to enhance thermal stability and coating properties. Detailed characterisation showed that LNPs interact with chitosan hydrogel through hydrogen bonding and electrostatic, as evidenced by FTIR spectroscopy. The thermal stability analysis revealed CsLNPs series with single-stage decomposition event and high T_{max} ranging from 285°C to 290°C, indicating their potential to withstand processing and storage conditions. However, some limitations were identified in this study. Introducing more than 10%wt LNPs induced agglomeration and uneven dispersion within the CsLNPs matrix. This agglomeration was initially beneficial by increasing thermal stability, but once a threshold was exceeded, further lignin loading reduced the overall thermal stability. Therefore, the matrix's degree of dispersion and uniformity should be further optimised in future studies to minimise agglomeration effects, which could negatively impact the material's mechanical properties and long-term stability. Additionally, while the thermal glass transition temperature Tg correlated well with T_{max}, further investigation is needed to assess the mechanical behaviour and long-term performance under various environmental conditions. Moreover, CsLNPs exhibited insoluble behaviour in non-polar solvents due to their inherent chemical structure, emphasising their potential as adequate moisture and toxic chemical compound barriers in food packaging. The increase in lignin loading up to 20% demonstrated enhanced water absorption capacity and slower degradation processes, highlighting the hydrophobic nature of lignin and its beneficial integration into chitosan matrices. Therefore, this work has already implemented sustainable usage and production of halal materials to address food safety and security challenges.

5. Author contributions

Conceptualization, MBHO and MNMI.; methodology, MBHO, AMAT and NNR.; software, AMAT and NNR.; validation, MBHO, MNMI and MSAS.; formal analysis, MBH Othman, AMAT and NRR.; investigation, MBHO, AMAT and NRR.; resources, MBHO.; data curation, MBHO, AMAT and NRR.; writing—original draft preparation, MBHO and AMAT;

writing—review and editing, MBHO and MSAS.; supervision, MBHO and MNMI; project administration, MBHO.; All authors have read and agreed to the published version of the manuscript.

6. Funding

This research was funded by a grant from the Ministry of Higher Education Malaysia, project number FRGS/1/2020/STG05/USM/02/3.

7. Institutional review board statement

Not applicable.

8. Data availability statement

The data are contained within this article.

9. Acknowledgements

We thank the School of Chemical Sciences, Universiti Sains Malaysia, for the technical support.

10. Conflicts of interest

The authors declare no conflicts of interest

References

Dong, Y., Ruan, Y., Wang, H., Zhao, Y., & Bi, D. (2004). Studies on Glass Transition Temperature of Chitosan with Four Techniques. Journal of Applied Polymer Science. https://doi.org/10.1002/app.20630

Hussin, M. H., Appaturi, J. N., Poh, N. E., Latif, N. H. A., Brosse, N., Ziegler-Devin, I., (2022). Recent Advancements in the Preparation, Characterisation, and Application of Nanolignin have been Made. International Journal of Biological Macromolecules. https://doi.org/10.1016/j.ijbiomac.2022.01.007

Islam, M. M., Shahruzzaman, M., Biswas, S., Nurus Sakib, M., & Rashid, T. U. (2020). Chitosan-based Bioactive Materials in Tissue Engineering Applications—A Review. Bioactive Materials. https://doi.org/10.1016/j.bioactmat.2020.01.012

Janik, W., Wojtala, A., Pietruszka, A., Dudek, G., & Sabura, E. (2021). Environmentally Friendly Melt-Processed Chitosan/Starch Composites Modified with PVA and Lignin. Polymers, 13(16), 1–14. https://doi.org/10.3390/polym13162685

Mohaiyiddin, M. S., Ong, H. L., Othman, M. B. H., Julkapli, N. M., Villagracia, A. R. C., & Md. Akil, H. (2018). Swelling Behaviour and Chemical Stability of Chitosan/Nanocellulose Biocomposites. Polymer Composites. https://doi.org/10.1002/pc.24712

Mohamad Zharif, Z., Nur Azira, T., & Muhamad Shirwan, A. S. (2021). Characterisation of L-cysteine Sources Using ATR-FTIR and Raman Spectroscopy. Halalsphere.

Munteanu, S. B., & Vasile, C. (2020). Vegetable Additives in Food Packaging Polymeric Materials. Polymers, 12(1), 28. https://doi.org/10.3390/polym12010028

Nasrollahzadeh, M., Ghasemzadeh, M., Gharoubi, H., & Nezafat, Z. (2021). Progresses in Polysaccharide and Lignin-Based Ionic Liquids: Catalytic Applications and Environmental Remediation. Journal of Molecular Liquids. https://doi.org/10.1016/j.molliq.2021.117559

Noor, N. M., Hashim, Y. Z. H.-Y., Sani, M. S. A., & Salim, W. W. A. W. (2020). Characterisation, Antibacterial and Anti-Inflammatory Activities of Electrospun Polyvinyl PVA Containing *Aquilaria Malaccencis* Leaf Extract ALEX Nanofibers. International Journal of Recent Technology and Engineering (IJRTE). https://doi.org/10.35940/ijrte.c4618.099320

Rafiae, N. N., Othman, M. B. H., Abdullah Sani, M. S., Mohamad Ibrahim, M. N., & Mohamad Daud, N. N. (2024). Preparation and Characterisation of Nano Lignin-Gelatine-Glycerol Composite (Nlggcs) Thin Film for Food Coating Application. Halalsphere. https://doi.org/10.31436/hs.v4i1.85

Rahman, O. U., Shi, S., Ding, J., Wang, D., Ahmad, S., & Yu, H. (2018). Lignin Nanoparticles: Synthesis, Characterisation and Corrosion Protection Performance. New Journal of Chemistry. https://doi.org/10.1039/c7nj04103a

Rai, S., Dutta, P. K., & Mehrotra, G. K. (2017). Lignin Incorporated Antimicrobial Chitosan Film into Food Packaging Applications. Journal of Polymer Materials.

Sekeri, S. H., Ibrahim, M. N. M., Umar, K., Yaqoob, A. A., Azmi, M. N., Hussin, M. H., (2020). Preparation and Characterisation of Nanosized Lignin from Oil Palm (*Elaeis Guineensis*) Biomass as a Novel Emulsifying Agent. International Journal of Biological Macromolecules. https://doi.org/10.1016/j.ijbiomac.2020.08.181

Sohni, S., Hashim, R., Nidaullah, H., Lamaming, J., & Sulaiman, O. (2019). Chitosan/nano-lignin based Composite as a New Sorbent for Enhanced Removal of Dye Pollution from Aqueous Solutions. International Journal of Biological Macromolecules.https://doi.org/10.1016/j.ijbiomac.2019.03.151

Souza, V. G. L., Pires, J. R. A., Rodrigues, C., Coelhoso, I. M., & Fernando, A. L. (2020). Chitosan Composites in Packaging Industry—Current Trends and Future Challenges. Polymers, 12(2), 417. https://doi.org/10.3390/polym12020417

Tang, Q., Qian, Y., Yang, D., Qiu, X., Qin, Y., & Zhou, M. (2020). Lignin-based Nanoparticles: A Review on their Preparations and Applications. Polymers, 12(11), 2471. https://doi.org/10.3390/polym12112471

Vågsholm, I., Arzoomand, N. S., & Boqvist, S. (2020). Food Security, Safety, and Sustainability—Getting the Trade-Offs Right. Frontiers in Sustainable Food Systems. https://doi.org/10.3389/fsufs.2020.00016

Vasilev, A., Efimov, M., Bondarenko, G., Kozlov, V., Dzidziguri, E., & Karpacheva, G. (2019). Thermal Behaviour of Chitosan as a Carbon Material Precursor Under IR Radiation. IOP Conference Series: Materials Science and Engineering. https://doi.org/10.1088/1757-899X/693/1/012002

Yaqoob, A. A., Sekeri, S. H., Othman, M. B. H., Ibrahim, M. N. M., & Feizi, Z. H. (2021). Thermal Degradation and Kinetics Stability Studies of Oil Palm (*Elaeis Guineensis*) Biomass-Derived Lignin Nanoparticle and its Application as an Emulsifying Agent. Arabian Journal of Chemistry. https://doi.org/10.1016/j.arabjc.2021.103182

Zhang, Z., Terrasson, V., & Guénin, E. (2021). Lignin Nanoparticles and their Nanocomposites. Nanomaterials, 11(5), 1336. https://doi.org/10.3390/nano11051336